

COMPARISON OF THE VISIBILITY OF LAMBERTIAN AND RETROREFLECTING OBJECTS

V.V. Barun

*B.I. Stepanov Institute of Physics,
Belarussian Academy of Sciences, Minsk, Belarus*

Received November 27, 1996

Image contrast and ultimate visibility range for Lambertian and retroreflecting objects observed through a light scattering medium are compared based on the small-angle approximation of the radiation transfer theory. The cases of an isolated object and an object against the background of an underlying surface are considered. It is shown, that the account for the signal coming from the shadow region of the isolated object can, under certain conditions, cause the maximum contrast at increasing optical thickness of the medium between an observer and Lambertian or retroreflecting object. The second case can also provide the maximum contrast for a retroreflector associated with its reflecting pattern and increase it efficient albedo. This peculiarity could be considered as one of the hypotheses explaining enhanced visibility of Earth's objects from the space. It is also shown that the dependence of the ultimate visibility range on the object albedo has a deep dip. When the Lambertian object albedo falls within a narrow range depending on the optical parameters of the medium, the small object becomes invisible over the whole scattering layer of a finite thickness because the object image contrast is below the threshold value.

The problem on investigation and optimization of the visibility characteristics is peculiar to the optics of scattering media and the image transfer theory. Many papers which estimate based on general criteria the efficiency of every concrete system in terms of minimizing optical noises, improving the image contrast, operation range and so on are devoted to solving this problem (see, for example, Refs. 1–4). Two points should be mentioned in connection with a great number of papers. First, the majority of these papers has analyzed the case of observation of Lambertian (or diffusely reflecting) objects. Second, even in the case of systems of Lambertian objects vision through scattering media investigated in detail some interesting in my opinion aspects drop out of the investigations. There are, for example, behavior of the object image contrast with its position within the layer of a finite optical thickness which is at first sight unexpected but can be simply explained in physical terms or the possibility to deduce simple analytical formulas estimating both contrast and visibility range.

There are precisely the questions to be addressed in the present paper. Lambertian objects and retroreflectors are chosen for a comparison. It is well known that the brightness of Lambertian objects does not depend on the observation direction, whereas retroreflectors reflect light exactly backwards. This choice is caused by at least two reasons. First, essential difference of the object reflection properties provides peculiarities of visibility characteristics to

be shown in more detail. The images of Lambertian and retroreflecting objects are easily expressible in an analytical form (see Refs. 5 and 8). Second, retroreflector are not only convenient for comparison but have wide application. The simplest example of a retroreflector is well known corner reflector. Retroreflectors or light returning (cataphoting) films and coatings are used in surface measurements of distances to artificial satellites and for communication with them (see Ref. 7), as passive reflectors in the systems of atmospheric pollution control by the method of differential absorption (see Ref. 8), for making traffic signs, advertisement panels, clearance indicators for heavy trucks (see Ref. 9), and so on.

Below we consider the visibility system of the "wide-narrow" type (see Ref. 1) which includes a radiation sources with a wide directional pattern (for example, the Sun at passive observation or diverged laser beam coming from a long distance) and a photodetector with narrow-angle sensitivity diagram (say, an eye in the case of visual observations).

Let us introduce, as usual, the location image contrast (see Refs. 2, 10):

$$k = (W_o - W_{\text{int}}) / W_{\text{int}} = W_{\text{vs}} / W_{\text{int}}, \quad (1)$$

where W_o is the signal power when the photoreceiver is oriented toward the object, W_{vs} and W_{int} are the signal power and optical noise, respectively. One can

see that conventional estimate of the signal as a difference of two signals entering the photodetector at its orientation toward the object and the background is used in Eq. (1). Necessary condition for the object visibility at a reasonably high radiation power, or what is the same, when the threshold signal-to-noise ratio is exceeded, is as follows:

$$|k| \geq k_{th}, \tag{2}$$

where k_{th} is the threshold contrast. Let us consider two examples of observation: 1) observation of an isolated object against the background of a scattering medium with, as a rule, finite optical thickness and “black” bottom; 2) an object against a Lambertian underlying surface with the albedo A_b . In the first case $W_{vs} = W(\tau_o) + W'_{bs}(\tau_o, \tau_1) - W_{bs}(\tau_1)$ and $W_{int} = W_{bs}(\tau_1)$,

$$k = \frac{W(\tau_o) - (1 - a) [W_{bs}(\tau_1) - W'_{bs}(\tau_o, \tau_1)] - a [W_b(\tau_o) - W'_b(\tau_o)]}{(1 - a) W_{bs}(\tau_1) + a [W_b(\tau_o) + W_{bs}(\tau_o)]}, \tag{3}$$

where $a = 0$ or 1 in the first and second case, respectively.

For the energy values entering into Eq. (3) to be calculated let us use the quasi-single scattering approximation (see Ref. 2). This means that we take into account multiple scattering as the radiation propagates from the sources in the forward direction, single scattering through high angle and once again multiple scattering as the radiation propagates backwards to the photodetector. Besides, let us identify direct (unscattered) light. Note that here we deal with the visibility problem when the medium optical thickness is not high, and, hence, consideration of the direct light is especially appropriate.

For the final expressions to be simplified and written in an analytical form the parameter $F(\tau_o) \varepsilon^2 \Sigma (F(\tau_o))$ (here $F(\tau_o)$ is the contribution of scattered light to the total light flux, Σ is the object geometric area) is assumed to be small as compared to the variance of the radial beam blooming $D_p(\tau_o)$ at the depth τ_o . Then designating by the indices « L » and « rr » Lambertian and retroreflecting objects, respectively, for the case of normal with respect to the layer boundary and the object surface illumination and observation in the backward direction one can obtain the following expressions (see Refs. 6, 11):

$$W_L(\tau_o) = (A_L / \pi) \exp[-(1 - \Lambda) \tau_o] \exp[-(1 - \Lambda) \tau_o], \tag{4}$$

$$W_{rr}(\tau_o) = [\beta(\tau_o) A_{rr} / \pi] \exp[-(1 - \Lambda) \tau_o] \exp[-(1 - \Lambda) \tau_o], \tag{5}$$

$$W_{bs}(\tau) = (\Lambda \bar{P} / 4\pi) \int_0^\tau S^2(\tau') d\tau' = (\alpha / \pi) \{1 - \exp[-2\tau(1 - \Lambda)]\}; \tag{6}$$

where τ_o and τ_1 are the optical thickness of the medium before the object on the illuminated side and total optical thickness of the light scattering layer, respectively ($\tau = \varepsilon z$, ε is the radiation decay, z is the geometric thickness); W is the signal power from the object itself, W'_{bs} is the power of the backscatter noise (PBN) when the photodetector is oriented toward the object with the account for shadowing of a medium portion by the object, W_{bs} is the PBN from the layer unperturbed by the object. In the second case $W_{vs} = W(\tau_o) + W'_b(\tau_o) - W_b(\tau_o)$, where $W'_b(\tau_o)$ and $W_b(\tau_o)$ are the background signal power entering the photodetector at its orientation toward the object and underlying surface, respectively. In this case Eq. (1) takes the following form:

$$W'_{bs}(\tau_o, \tau_1) = W_{bs}(\tau_1) - (\Lambda \bar{P} / \pi) \int_{\tau_o}^{\tau_1} S(\tau) S(\tau - \tau_o) \exp(-\tau_o) d\tau, \tag{7}$$

where A_L and A_{rr} are albedo of the objects; $\Lambda = \sigma / \varepsilon$ is the photon survival probability; σ is the scattering coefficient; $\beta(\tau_o) = \exp\{-\delta^2 / [8D_{\rho\theta}(\tau_o)]\} / [8D_{\rho\theta}(\tau_o)]$ is the “coefficient of amplification” for the retroreflecting object (see Refs. 5, 6); δ is the angle between the optical axis of the source and photodetector; $D_{\rho\theta}(\tau_o)$ is the variance of the angular blooming of the beam from narrow-angle source which

is equivalent to the photodetector (see Refs. 5, 6); \bar{P} is the average value of the backscattering phase function; $\alpha = \Lambda \bar{P} / [8(1 - \Lambda)]$ is the luminance factor of semi-infinite layer; $S(\tau) = \exp[-(1 - \Lambda) \tau]$ is the normalized total radiation flux at optical thickness τ in the small-angle approximation (see Ref. 2). Below the angle δ is assumed to be small but nonzero, which allow us to “tune out” from the retroreflected glare in the same manner as specularly reflected component or “sun track” are removed in the case of observation of smooth surface of the water. The second term in Eq. (7) with sign “-” shows that a small object removes from its shadow region both unscattered radiation from the narrow-angle fictitious source and the light which comes to the object directly and then would converted into scattered radiation in the medium behind the object.

First we consider the image contrast of isolated Lambertian object which is observed against the background of the scattering medium layer ($a = 0$ in Eq. (3)). This medium is modeled by Cloud C-1 (see Ref. 12) with the following optical parameters: $\Lambda = 0.87$, $\bar{P} = 0.64$ and mean-square value of the

scattering angle $\beta_2 = 0.07$. As it is usually made in the small-angle approximation of the radiation transfer theory (see Ref. 2), deviation of Λ from 1 accounts for the radiation scattered at high angles ($\geq 45^\circ$) to be assigned to the absorbed one. By substituting Eqs. (4), (6) and (7) into Eq.(3) we can verify that function $k(\tau_o)$ reaches an extremum at the optical depth of:

$$\tau_o^* = \tau_1 + \frac{1}{2(1-\Lambda)} \ln \left[\frac{2-\Lambda}{\Lambda} (1 - A_L/\alpha) \right]. \quad (8)$$

This extremum is a maximum located within the layer $0 < \tau_o^* < \tau_1$ if and only if $A_1^* < A_L < A_2^*$, where $A_1^* = \Lambda \bar{P} / [4(2-\Lambda)]$, $A_2^* = \alpha \{1 - [\Lambda / (2-\Lambda) \exp[-2\tau_1(1-\Lambda)]]\}$. If A_L is close to A_1^* , maximal contrast k_{Lmax} occurs in the vicinity of the rear boundary of the layer $\tau_o^* \approx \tau_1$, whereas at $A_L \approx A_2^*$ $\tau_o^* \approx 0$, that means that the maximum correspondingly shifts within the medium (see curves 2 and 3 in Fig. 1). From Eq. (3) and Eq. (8) we can derive that

$$k_{Lmax} = \frac{2(1-\Lambda)}{2-\Lambda} \frac{\exp[-(2-\Lambda)\tau_1]}{1 - \exp[-2(1-\Lambda)\tau_1]} X^{-\Lambda/[2(1-\Lambda)]}, \quad (9)$$

where $X = [(2-\Lambda)/\Lambda] (1 - A_L/\alpha)$. It is seen that always $k_{Lmax} > 0$. As shown in Fig. 1, the following visibility conditions can take place in accordance with the object albedo A_L and optical thickness τ_1 :

1. If $A_L > A_2^*$, the contrast $k(\tau_o) > 0$ within the layer at any τ_1 and decreases as τ_o increases (see curve 1 in Fig. 1). This is usual behavior of $k(\tau_o)$.

2. As mentioned above, if $A_1^* < A_L < A_2^*$, the contrast has a maximum within the layer. At small τ_o , contrast $k(\tau_o)$ increases with τ_o increase, while its sign (and, hence, improvement or deterioration of the object visibility) depends on the albedo A_L and optical parameters of the medium. If $A_L \geq A_3^* = \alpha \{1 - \exp[-2\tau_1(1-\Lambda)]\} > A_1^*$ (the latter inequality is equivalent to the following requirement $\tau_1 > \tau_1^* = \{1/[2(1-\Lambda)]\} \ln(2/(\Lambda-1))$, $k(\tau_o) \geq 0$ and the object visibility improves with τ_o increase during its "sink" into the layer starting at the illuminated boundary (see curve 2 in Fig. 1). At $A_L < A_3^*$ contrast is negative at small optical depth. Then, the object disappears in the vicinity of $\tau_o^{**} = \tau_1 + 1/[2(1-\Lambda)] \ln(1 - A_L/\alpha)$ because the condition (2) does not hold, then it appears again at contrast $k > 0$. The latter has a weak maximum (see curve 3 in Fig. 1). From Eq. (9) one can estimate ultimate values of the layer optical thickness τ_1^{**} and the object albedo A_L^* when maximum contrast of the object is above the threshold level. Substituting Eq. (9) into Eq. (2) with the account for $A_L < A_2^*$ gives

$$\tau_1 < \tau_1^{**} = \frac{1}{2(1-\Lambda)} \ln \left[1 + \frac{2(1-\Lambda)}{k_{th}(2-\Lambda)} \right], \quad (10)$$

$$A_L > A_L^* = \alpha \times$$

$$\times \left\{ 1 - \frac{\Lambda}{2-\Lambda} \left[\frac{2(1-\Lambda) \exp[-(2-\Lambda)\tau_1]}{k_{th}(2-\Lambda)(1 - \exp[-2\tau_1(1-\Lambda)])} \right]^{2(1-\Lambda)/\Lambda} \right\}. \quad (11)$$

This means that if the inequalities (10) and (11) are fulfilled simultaneously, we have Eq. (2).

3. If $A_L < A_1^*$, contrast increases monotonically over the layer and reaches its positive peak at the rear boundary of the medium $\tau_o = \tau_1$. The sign of k at small τ_o depends on A_L and τ_1 in the same manner as described in Sect 2. As $A_3^* \leq A_L \leq A_1^*$, $k \geq 0$, otherwise contrast is negative and increases with τ_o . In the vicinity of $\tau_o = \tau_o^{**}$ and taking into account that $|k| < k_{th}$ the object is invisible, then it appears with positive contrast (see solid curve 4 in Fig. 1).

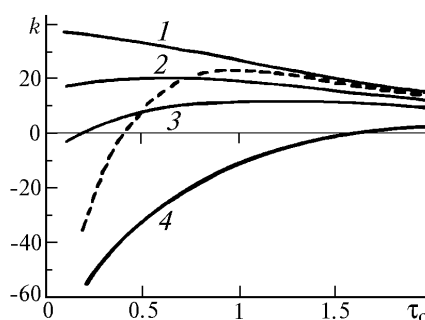


FIG. 1. Dependence of $k(\tau_o)$ in percent in the case of observation of an isolated Lambertian object (solid curves) and retroreflector (dotted curves) through a model scattering medium Cloud C-1 with the following optical parameters: $\Lambda = 0.87$, $\bar{P} = 0.64$ and $\beta_2 = 0.07$ for $A_{L,rr} = 0.3$ (curve 1), 0.25 (curve 2), 0.2 (curve 3), and 0.05 (curve 4), $\tau_1 = 2$.

Using Eq. (3) one can estimate the range of optical thickness where the object becomes invisible. Actually, expanding $k(\tau_o)$ into a Taylor series in the vicinity of $\tau_o = \tau_o^{**}$ and considering only linear terms we can obtain the following expression:

$$\Delta\tau = \frac{k_{th}}{a(1-\Lambda)} \exp[(2-\Lambda)\tau_1] \times \{1 - \exp[-2\tau_1(1-\Lambda)]\} \left(\frac{a - A_L}{a} \right)^{\Lambda/[2(1-\Lambda)]}. \quad (12)$$

Unusual behavior of $k(\tau_o)$, namely, the increase of the contrast with the medium optical thickness in front of the object considered in Sects. 2 and 3, is observed not only for Lambertian objects. For example, qualitatively similar peculiarities of $k(\tau_o)$ can be obtained for retroreflector (see dotted curve 4 in Fig. 1). In this case in addition to the consideration of the signal from the object shadow area peculiarities associated with the specific radiation reflection from the surface are evident. For instance, this causes higher compared to Lambertian object contrast increasing at a higher rate with

increasing τ_o , the maximum to be sharper, the range of optical thickness where the object becomes invisible due to a failure of Eq. (2) to be narrowed and so on.

For retroreflector (and, in general, for the object with an arbitrary coefficient of brightness) observations substitution Eq. (5) in Eq. (3) could give expression similar to Eqs. (8)–(11) and the visibility condition of such an object being similar to those presented above could be considered. However, all parameters (τ_o^* , A_1^* and so on) could be expressed by the solutions of corresponding transcendental equations or inequalities. Therefore to avoid complexity we do not make this procedure.

In fact, when deriving well-known formula for the meteorological visibility range (MVR) $S_m = -(1/\epsilon) \ln k_{th} = 3.91/\epsilon$ at $k_{th} = 0.02$ the shadowing of the medium by a small object is also considered. For the condition of MVR measurement (observation of a black body along a horizontal path at $\tau_1 \rightarrow \infty$) when inequality (3) is yet valid the following ultimate value of the optical thickness is simple to estimate:

$$T_o = \epsilon S'_m = [1/(\Lambda - 2)] \ln k_{th}. \tag{13}$$

This expression reduces to a conventional formula for MVR at $\Lambda = 1$. The presence of the factor $1/(\Lambda - 2)$ in Eq. (13) derives from the fact that for the active visibility system considered in this paper illuminance of the object depends on τ_o , whereas for the MVR measurement scheme illuminance is constant. In our case the constancy is achieved at $\Lambda = 1$. The normalized light flux $S(\tau_o)$ incident on the object is in this case equal to 1 at any τ_o , so that the above equality $S_m = S'_m$ is valid.

Let us now consider the case when retroreflecting object placed on Lambertian underlying surface is observed and they both are “immersed” into a scattering medium. For instance, this situation can be achieved for cataphotic traffic sign applied on Lambertian base as the optical thickness between the sign and an observer increases. As seen from Eq. (5), in that case (see Refs. 5 and 6) small retroreflector can be replaced by a Lambertian object with the efficient albedo $A_{ef} = \beta(\tau_o) A_{rr}$ increasing with increasing τ_o when τ_o is small and which value can be significantly greater than 1. Thus, two processes influencing the contrast in opposite directions are compete during the retroreflector image formation. First process is connected with the increase of A_{ef} at small τ_o and corresponding rise of k , while the second one is related to extinction of signal and increase of the MVR, causing k to decrease (see Eq. (3)). Joint action of these processes determines dependences presented in Fig. 2, where the case of normal illumination of a small retroreflector and its observation (also normally to the common plane of the object and the background and to the medium boundary) through the layer of scattering medium against the background of Lambertian surface with $A_b = 0.3$.

Comparison of the dependences presented in Figs. 1 and 2 shows that they, not only qualitatively, have common characteristics, but significant distinctions, as well. For instance, because of the above mentioned “tuning off” from the retroreflector grazing the retroreflector contrast at the upper boundary of the layer is always negative and equal to -1 . With increasing τ_o the object visibility declines, then the object disappears as the condition Eq. (2) violates and at corresponding albedo A_{rr} can again become visible with the positive contrast (even at $A_{rr} < A_b$) which reaches its peak (see curves 2 and 3). In this case there is no upper limit on A_{rr} as it is for an isolated Lambertian object. The range of τ_o at which the object disappears is narrower as compared to that presented in Fig. 1. The peak of $k(\tau_o)$ presented in Fig. 2 is sharper while its position is more stable as compared to those presented in Fig. 1 and depends only weakly on A_{rr} . Here, as in the remark to Fig. 1, all parameters similar to those given by Eqs. (8)–(11) can be easily expressed by the solution of transcendental equations and inequalities. Note also that the image contrast of a Lambertian reflector placed on the background of underlying surface depends on τ_o in a usual way. This means that $|k(\tau_o)|$ decreases as τ_o decreases and the object visibility is progressively poorer while the values of k themselves are positive at $A_L > A_b$, otherwise being negative.

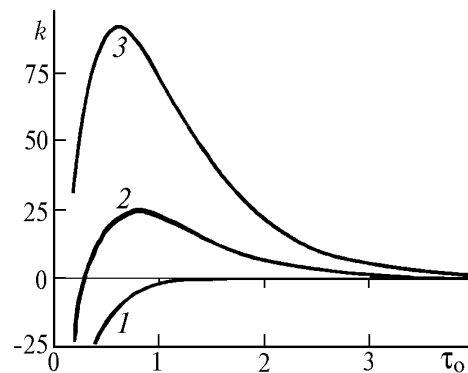


FIG. 2. Dependence of $k(\tau_o)$ in percent in the case of observation of a retroreflector against the background of Lambertian surface with $A_b = 0.3$ through a model scattering medium, Cloud C-1 at $A_{rr} = 0.05$ (curve 1), 0.1 (curve 2), and 0.2 (curve 3).

Let us consider one more interesting case of the observation which is illustrated in Fig. 2. Imagine that the image of a surface object is formed through the atmosphere with an airborne or a spaceborne system flying a different heights. As is evident from the data presented in Fig. 2, it may happen that the object visibility is better from large height than from a low one. Thus the presence of some fraction of retroreflected radiation can be proposed as a hypothesis for the reason of improving visibility of Earth’s objects from the space. Nevertheless, further

investigations and extended calculations are needed to justify this hypothesis. Note that the specular fraction in the reflected light could also cause the object image contrast to increase with increasing τ_0 , as well. However consideration of this problem is beyond the scope of this paper.

The quantitative dependence of the image contrast obtained above allow us to consider ultimate range of vision of an object for two cases to be investigated here. This problem has been partially touched in the above remark concerning the MVR measurements. The ultimate visibility range (or corresponding ultimate optical thickness T_0^* is, by definition, the maximum distance between an

observer and an object which yet provides threshold (or minimal) contrast k_{th} or, what is the same, gives solution to the following equation: $|k(T_0^*)| = k_{th}$. This parameter is frequently considered to be the main in a comparison and estimates of the advantages and disadvantages of different systems for vision through a scattering medium. Dependence of T_0^* ($A_{L,rr}$) for the case of observation of an isolated object (a) and an object on the background of underlying surface with albedo $A_b = 0.3$ (b) at different optical thickness of a layer τ_1 and $k_{th} = 0.02$ are presented in Fig. 3. In either case a deep fall in $T_0^*(A_{L,rr})$ observed within a relatively narrow range of the object albedo attracts our attention.

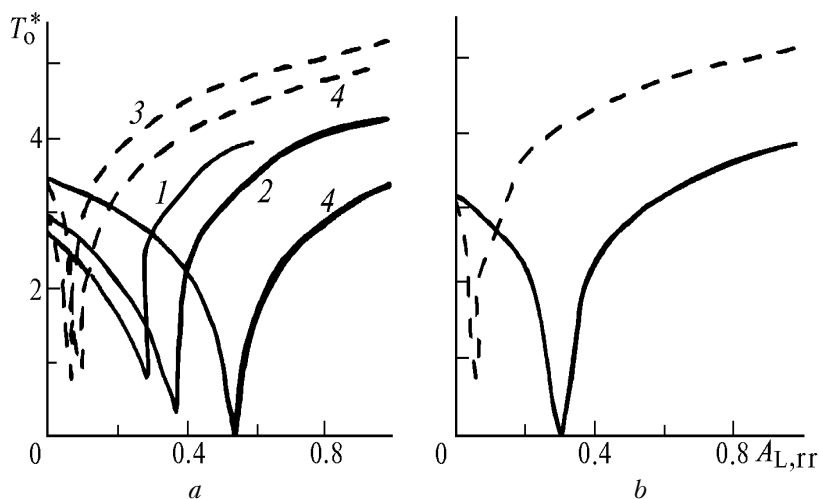


FIG. 3. Ultimate optical thickness T_0^* versus albedo of an isolated object at $\tau_1 = 4$ (curve 1), 5 (curve 2), 6 (curve 3) and for a semi-infinite layer (curve 4) of the model scattering medium Cloud C-1 (a) and that for a Lambertian object (solid curves) and retroreflector (dotted curves) against the background of underlying surface with $A_b = 0.3$ for (b).

First we consider the solid curves presented in Fig. 3a, which correspond to a Lambertian reflector. As τ_1 increases, minimal optical thickness decreases. Eventually, beginning with some τ_1 the object with albedo in a narrow range becomes invisible throughout the whole layer of scattering medium starting with its illuminated boundary. Equation (3) can make sure that there is the range of albedo A_L where $|k|$ does not exceed threshold contrast even at $\tau_0 = 0$ (as is seen from Eq. (8), in this case $W'_{bs}(\tau_0, \tau_1) = 0$). $T_0^*(A_L)$ is minimal within a narrow region in the vicinity of $A_L \approx A_L^*$, whereas position of this minimum shifts only slightly as τ_1 increases in the range from zero to the brightness coefficient α of a semi-infinite layer. Such a peculiarity of the ultimate visibility range within this layer is quite obvious and can be easily examined by direct substitution of Eqs. (4), (6) and (7) in Eq. (3) keeping in mind that $A_L^* = \alpha$. Nevertheless, it is rather unexpected for the layer with a finite (and moderately high) optical thickness. Dependences of $T_0^*(A_{rr})$ for a retroreflector (see dotted curves) also

have a minimum and their position is more stable as compared to that for a Lambertian object observation.

The action of the changes in efficient albedo itself is well seen in Fig. 3b (dotted line), where only optical thickness of the medium before the object and its base is of importance while the signal from the shadowed region is nil. If for a Lambertian object minimal (zero) value of T_0^* is apparent and takes place at $A_L = A_b$, in the case of a retroreflector its A_{ef} approaches A_b at some depth $\tau_0 = T_0^*$ corresponding to the minimal ultimate visibility range.

In conclusion it should be pointed out that in this paper we have analyzed and quantitatively estimated for the case of small Lambertian objects or retroreflectors the parameters explaining "untraditional" behavior of the object image contrast versus optical thickness of the medium through which the observations are made. Here increase of the contrast with increase τ_0 increase and its peaking is considered as "untraditional". Everyday experience makes us to expect that the thicker is the layer of a turbid medium against the object, the more bloomed

is its image, and, at the first sight, the answer to the question of whether k can increase with increasing τ_0 should be negative. However, as it follows from the above consideration, this is not always true. The peculiarities considered in the present paper must be taken into account when solving different problems on the image analysis and reconstruction of an object characteristics from its image.

REFERENCES

1. D.M. Bravo-Givotovsky, L.S. Dolin, A.G. Luchinin, and V.A. Savelev, *Izv. Akad. Nauk SSSR, Fiz. Atmos. Okeana* **5**, No. 7, 672–684 (1969).
2. E.P. Zege, A.P. Ivanov, and I.L. Katsev, *Image Transfer in Scattering Medium* (Minsk, 1985), 328 pp.
3. O.A. Sokolov, *Visibility under the Water* (Leningrad, 1974), 232 pp.
4. J.S. Jaffe, *IEEE J. Oceanic Eng.* **15**, No. 2, 101–111 (1990).
5. V.V. Barun, *Proc. SPIE* **2410**, 470–480 (1995).
6. V.V. Barun, *Opt. Eng.* **35**, No. 7, 1894–1900 (1996).
7. P.A. Lightsey, *Opt. Eng.* **33**, No. 8, 2535–2543 (1994).
8. H. Edner, P. Rasnarson, and S. Srahmare, S. Svanberg, *Appl. Opt.* **32**, No. 3, 327–337 (1993).
9. V.F. Kutenev and B.V. Kisulenko, *Standartization and Certification in Motor Industry*, Trudi NAMI, 3–12 (1993).
10. I.L. Katsev and E.P. Zege, *Izv. Akad. Nauk SSSR, Fiz. Atmos. Okeana* **25**, No. 7, 732–740 (1989).
11. V.V. Barun, *Proc. SPIE* **2759**, 490–501 (1996).
12. D. Deirmendjian, *Electromagnetic Scattering on Spherical Polydispersions* (American Elsevier, New York, 1969).